Cancer Chemother Pharmacol (2009) 64:1047–1052
DOI 10.1007/s00280-009-1082-x

ORIGINAL ARTICLE

The acute effects of CMF-based chemotherapy on maxillary periodontal microcirculation

Dan M. J. Milstein · Rick Bezemer · Jérôme A. H. Lindeboom · Can Ince

Received: 4 May 2009 / Accepted: 9 July 2009 / Published online: 25 July 2009

Abstract
Purpose A high incidence of oral complications is associated with chemotherapy (CT) treatment in cancer patients; however, while knowledge into molecular mechanisms of their pathobiology continue to evolve, the direct physiological effects of CT on oral tissue perfusion remain unexplored. The aim of this investigation was to assess the acute effects of CT on gingival microcirculation perfusion by measuring gingival capillary density.
Methods Twenty female specific-pathogen free New Zealand White rabbits were randomly divided into four groups receiving four different intravenous dose levels of cyclophosphamide, methotrexate, and fluorouracil (CMF). Noninvasive measurements of gingival capillary density were performed using sidestream dark-field (SDF) imaging prior to and 30 min after CT treatment. Four rabbits receiving saline solution were used as control animals.
Results Baseline gingival capillary density was 58 ± 11 cpll/mm^2, no significant differences in baseline capillary densities between the groups were found. From low to high dose CT, capillary density 30 min after CMF treatment increased in each group by 1 ± 7, 5 ± 7, 13 ± 18 and 20 ± 13 cpll/mm^2, respectively. Capillary density increase was significant in the high-dose group. No change in gingival capillary density was found in the control group.
Conclusions Periodontal microcirculation perfusion had increased 30 min after CT treatment as indicated by a rise in gingival capillary density. Our results support the idea that CT-induced microcirculatory response not only diligently delivers but also saturates peripheral oral tissues with antineoplastic agents by increasing surface area exposure. This functional response of the microcirculation to CT drugs may play a role in contribution to oral complications and the treatment of oral tumors.

Keywords Capillary density · Chemotherapy · Gingiva · Microcirculation · SDF imaging

D. M. J. Milstein (✉) · R. Bezemer · C. Ince
Department of Translational Physiology,
Academic Medical Center, University of Amsterdam,
Meibergdreef 9, 1105 AZ Amsterdam, The Netherlands
e-mail: D.M.Milstein@amc.uva.nl; D.M.Milstein@amc.nl

D. M. J. Milstein · J. A. H. Lindeboom
Department of Oral and Maxillofacial Surgery,
Academic Medical Center, University of Amsterdam,
Meibergdreef 9, 1105 AZ Amsterdam, The Netherlands

D. M. J. Milstein · J. A. H. Lindeboom
Academic Centre for Dentistry Amsterdam (ACTA),
University of Amsterdam, Louwesweg 1,
1066 EA Amsterdam, The Netherlands

Introduction

Chemotherapy (CT) has greatly improved the outcome of cancer patients and is a mainstay for management of many types of malignant neoplasms. However, a high incidence of oral complications is associated with CT in cancer patients [18] and despite ongoing research into the complex pathobiology of these clinical side effects at the cellular and molecular level, no information currently exists depicting the changes in oral microcirculation during cytostatic treatment. Hence, direct observation and quantification of functional changes in the oral microcirculation in relation to CT could provide useful information on the effects of antineoplastic agents on mucosal perfusion and its possible contributions to CT-associated oral complications.

Previous studies, focusing on changes in oral microcirculation in dentistry and oral medicine have used a non-invasive intravital imaging technique known as orthogonal polarization spectral (OPS) imaging [13–15]. Recently an improved imaging technique was introduced by our group called sidestream dark-field (SDF) imaging [10], which is currently being used in many animal and clinical studies [3, 4, 16, 19, 21, 22] directed at exploring the clinical significance of changes in microcirculation density and perfusion.

The aim of this study was to test the hypothesis that microcirculatory alterations occur as an early response to CT. We developed an animal model to measure the dose-dependent effects of CT on gingival microcirculation perfusion by measuring gingival capillary density prior to and 30 min after CT intervention using SDF imaging.

Methods

Animals

This study was reviewed and approved by the institutional Animal Experimentation Committee of the Academic Medical Center of the University of Amsterdam. Twenty-four female specific-pathogen free (SPF) New Zealand White rabbits (Harlan Netherlands BV, Horst, The Netherlands) with a mean body weight of 3.0 ± 0.6 kg were used in this study. The animals were housed in pairs in large conventional cages in a light-controlled room kept at 22 ± 1°C with a relative humidity of 55 ± 10% and received commercial feed pellets and water for consumption ad libitum. All animals received a subcutaneous injection of ketamine hydrochloride (Ketamine, Alfasan International BV, Woerden, The Netherlands; 15.0 mg/kg) and medetomidine hydrochloride (Domitor®, Pfizer Animal Health BV, Capelle aan den Ijssel, The Netherlands; 0.2 mg/kg) to achieve sedation for capillary density measurements and administration of CT drugs. An intravenous (IV) line was introduced into the marginal ear vein for the indicated interventions; CT and 0.9% NaCl (saline) solution as described below. After administering the designated interventions and measuring capillary density, the IV line was withdrawn and an intramuscular injection of atipamezole hydrochloride (Antisedan®, Pfizer Animal Health BV, Capelle aan den Ijssel, The Netherlands; 1.0 mg/kg) was administered to antagonize sedation.

Interventions

Based on clinically relevant antineoplastic therapy for metastatic breast cancer from literature [1, 5, 6, 12] using cyclophosphamide (600 mg/m^2), methotrexate (40 mg/m^2) and fluorouracil (600 mg/m^2) (CMF), we initiated an allometric analysis to determine CMF drug posologies for the rabbit. To our knowledge, no drug dosages reflecting CMF polychemotherapy used in routine clinical practice have previously been described for systemic administration in the rabbit. An allometric equation relating metabolic rate and body weight was used: $Y = a \cdot W^b$, where Y represents metabolic rate of the species of interest, a is a taxonomically dependent constant (allometric coefficient for placental mammals is 70), W is mass in kilograms (60 kg for human and 3 kg for rabbit) and b is the allometric exponent (0.75) [7, 9]. The animal groups were categorized according to different dose levels of CMF as follows; allometric dose (AD, $n = 4$), half of allometric dose (HD, $n = 4$), a third of the allometric dose (TD, $n = 4$), quarter of the allometric dose (QD, $n = 8$) and no CMF (control, $n = 4$).

Table 1 summarizes the treatment groups, drug dosages and their corresponding animal populations. CMF CT, cyclophosphamide (CTX) (Endoxan®, Baxter BV, Utrecht, The Netherlands), methotrexate (MTX) (Emtrexate®, Pharmachemie BV, Haarlem, The Netherlands) and fluorouracil (5-FU) (Fluorouracil, TEVA Pharma BV, Mijdrecht, The Netherlands), or 0.9% NaCl solution was administered for 3 min intravenously in each animal. During the sequential administration of CTX, MTX, and 5-FU, a total of 4.0 ml of sterile saline solution was distributed evenly between each cytostatic drug bolus. For the control animals, saline solutions equivalent to CMF plus 4.0 ml was administered.

Microcirculation imaging technology

Gingival microcirculation imaging was performed using SDF technology (Microscan Video Microscope System, MicroVision Medical, Amsterdam, The Netherlands) [8, 10, 17]. This noninvasive intravital imaging technique is incorporated into a handheld video microscopy instrument and operates by illuminating the tissue of interest using concentrically positioned light emitting diodes (LEDs) placed around the exterior tip of a central light guide. In this way, the illuminating light source is optically isolated from the detection light path in the core of the light guide, thus preventing image contamination by tissue surface reflections. The LEDs emit light at a wavelength of 530 nm, which corresponds to an isosbestic point in the absorption spectra of oxy- and deoxyhemoglobin. By using this wavelength, sufficient optical absorption by hemoglobin in the red blood cells is ensured regardless of oxygenation state. All imaging was performed using a 5× objective that was captured by video camera with a 720 × 576 pixel resolution, resulting in a 1.0 × 0.75 mm imaged tissue segment. All measurements were recorded

Table 1 Summary of study groups, interventions, drug dosages, and animal populations

Groups	Interventions	CTX (mg/kg)	MTX (mg/kg)	5-FU (mg/kg)	No of animals
CTRL	0.9% NaCl	–	–	–	4
QD	CMF	8.6	0.6	8.6	8
TD	CMF	11.4	0.8	11.4	4
HD	CMF	17.2	1.2	17.2	4
AD	CMF	34.3	2.3	34.3	4

CTRL control, *QD* quarter allometric dose, *TD* third allometric dose, *HD* half allometric dose, *AD* allometric dose, *CTX* cyclophosphamide, *MTX* methotrexate, *5-FU* fluorouracil

for 1 min on a Sony SDR-20P DVCAM video recorder (Sony, Shinagawa-ku, Tokyo, Japan) and viewed on a Sony PVM-97 black-and-white video monitor (Sony, Shinagawa-ku, Tokyo, Japan).

SDF measurements

Once anesthetized, each rabbit was restrained in a sternally recumbent position into a tabletop rodent mouth gag apparatus (Veterinary Instrumentation Limited, Sheffield, South Yorkshire, United Kingdom) with the jaws fixed in an open configuration (Fig. 1a). Designed to fit aptly under the hard palate, the maxillary incisor teeth were positioned over the upper bar of the table restrainer and the mandibular incisors were anchored under the lower bar. The mouth was then opened by gently lifting the upper bar and fixing it into position using two small lateral screws. Using an additional screw, mandibular extension was adjusted carefully to prevent excessive stretching of masticatory muscles and articular ligaments. To reduce both stress on the neck and back muscles and excessive traction on the incisor teeth, the restrainer platform was tilted to 30° [2].

The SDF device was mounted on a micromanipulator to ensure stable positioning of the imaging probe during image acquisitions. Measurements were performed by gently placing the lens of the probe, covered with a sterile disposable cap (Microscan Lens, MicroVision Medical, Amsterdam, The Netherlands) on the anterior maxillary incisor gingiva (Fig. 1b). Microcirculation imaging was performed prior to and 30 min after CT or saline interventions. For both time points, two 30-s recordings were captured. By withdrawing the SDF imaging probe briefly between these two image recordings, we ensured no pressure artifacts were present during image acquisition. From these two recordings, two video frames were isolated using Adobe Premier Pro 1.5 (Adobe Systems Incorporated, San Jose, California, USA) for offline analysis of gingival capillary density. Figure 1c illustrates the complete experimental setup during data acquisition.

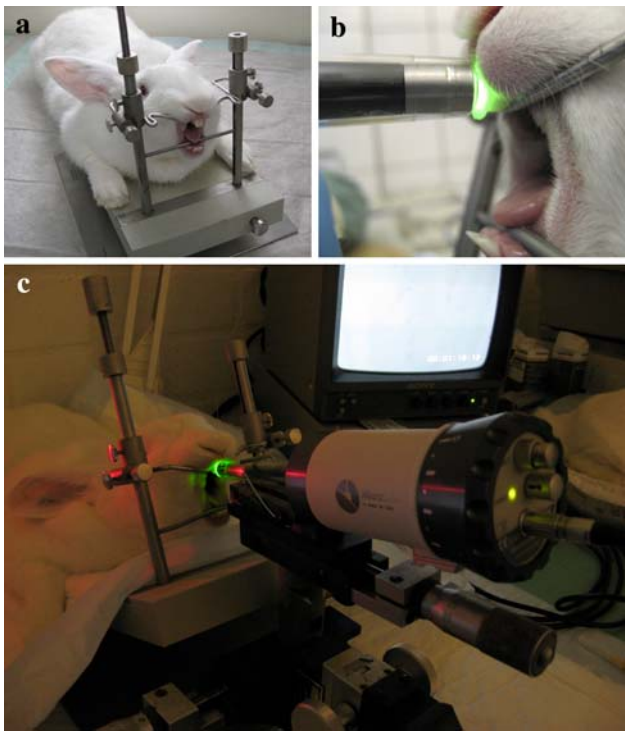

Fig. 1 Rabbit restrained in tabletop mouth gag apparatus (**a**), positioning of imaging probe on rabbit maxillary incisor gingiva (**b**), and experimental setup during acquisition of gingival microvascular measurements using sidestream dark-field imaging (**c**)

Microcirculation image analysis

Offline image analysis of gingival capillary density was performed by counting the number of perfused capillaries in each frame; the area of an SDF image frame, consisting of gingival tissue and adjacent dental structures, was 0.75 mm^2. After counting capillary density on the computer screen, gingival surface dimensions were digitally calculated in each frame using Adobe Photoshop CS3© (Adobe Systems Incorporated, San Jose, California, USA). Quantification of gingival capillary density for each group was expressed as the mean number of capillaries ± SD per millimeter squared (cpll/mm^2).

Statistical analysis

Data analysis was performed using GraphPad Prism version 5.0 for Windows (GraphPad Software Inc., La Jolla, California, USA). Comparative analysis of gingival capillary density between time points and the study groups was performed using analysis of variance with a Bonferroni post hoc test and the paired *t* test. A receiver operator characteristic (ROC) curve was used to determine a predictive value on outcome related to changes in gingival capillary density after 30 min of CT intervention and the

area under the curve (AUC) was computed. Differences between groups with a P value less than 0.05 were considered statistically significant. All data are presented as mean ± SD.

Results

The gingiva was easily accessible and provided enough contrast for the capillaries to be clearly visible and easily counted (Fig. 2). Baseline mean gingival capillary density was 58 ± 11 cpll/mm^2, no significant differences in baseline capillary densities between the groups were found. Thirty minutes after CT treatment gingival capillary density had increased by 5 ± 7, 13 ± 18 and 20 ± 13 cpll/mm^2, respectively, in the TD, HD, and AD groups. Gingival capillary density in the control and QD groups remained unchanged. Figure 3a illustrates the changes in gingival capillary density in each group. Capillary density increase was significant in the AD group (paired t-test, $P < 0.05$ for 30 min vs. baseline), but not in the other groups. In comparison to control and the QD group, the increase in the AD group was significantly higher (one way ANOVA, $P < 0.05$ for AD vs. control and QD). Consequently, CMF only had a significant effect in the AD group. All control and QD group animals survived the protocol, while the animals in the TD, HD, and AD groups died overnight. Figure 3b illustrates the changes in gingival capillary density in the control, surviving and non-surviving animals. A ROC curve (Fig. 4) showed that changes in gingival capillary density after 30 min of CT intervention was a good predictor of mortality in our animals (AUC = 0.952, $P < 0.002$).

Discussion

The aim of the present investigation was to test the hypothesis that microcirculatory alterations occur as an early response to CT by measuring gingival capillary density. This study is unique as it attempts to noninvasively quantify gingival microcirculatory changes in vivo as a result of CT. Our results show that gingival capillary density had increased 30 minutes after IV administration of CT. CMF drug doses from the TD, HD, and AD groups showed an acute effect on gingival microcirculation and higher doses of CT significantly altered the microcirculation and resulted in death of the animals.

The design of the present investigation offered the possibility of validating our allometric drug calculations by testing if our CMF posologies yielded results sensitive enough for the chosen animal species. To our knowledge, no systemic CMF models in rabbits have been reported which depict the relevance of CMF combinations used in humans [1, 5, 6, 12] on oral microcirculatory networks. The scaled CMF drug concentrations in the AD, HD, and TD groups were sufficiently high to induce changes in gingival microcirculation. Scaling CMF-based CT from human to rabbit resulted in lower drug dosages for CTX, MTX, and 5-FU in the rabbit in comparison to other studies which have used single agents (CTX and 5-FU) at higher dose levels [11, 20]. Those studies reported a high incidence in animal mortality as a result of cardiotoxicity from high-dose CTX or 5-FU, in the present study at lower concentrations the CMF combination resulted in the same fate in our animals, indicting their toxicity potential even at lower drug concentrations. Interestingly, a correlation between microcirculation and mortality was observed which indicated a possibility of predicting survival outcome by interpreting capillary density in vivo in an early dose-response phase. Acute precapillary vasodilation with subsequent recruitment of preexisting gingival microvessels can explain the observed increase in gingival capillary density in our model and thereby demonstrating acute vascular regulation properties of antineoplastic drugs. With a mortality rate of 60% in our CT groups, the best cutoff chosen in the ROC curve had a sensitivity of 83% and a specificity of 100%, indicating that changes in gingival capillary density greater than 10.5 cpll/mm^2 was directly proportional to a lethal outcome from CMF.

The oral and maxillofacial compartments are highly vascularized and offer unique approachable locations for monitoring and quantifying the microcirculation. We selected the anterior maxillary interdental gingiva since the tissue dimensions were small and easily accessible. Using SDF imaging, we were able to quantify gingival capillary density in situ without the need for destructive tissue preparations or invasive procedures while producing good image quality with enough contrast for the microcirculation to be readily visible. The changes in gingival perfusion demonstrated by the rise in gingival capillary density resulted in increased tissue perfusion with subsequent drug delivery. To this end, the observed effect of CT on the microcirculation in our study may actually indicate a beneficial role of microvascular networks as they promote the ability of the antineoplastic agents to exert their pharmacological effects across larger surface areas in different tissue compartments. By investigating microcirculatory response as a result of anti-cancer treatment, important insight into the working mechanisms of CT on vascular and microvascular regulation can be scrutinized. Furthermore, translating the results from the present study into clinical significance, the observed effect of CT on microvascular networks may be the culprit mechanism responsible for extending exposure and transudation of toxic CT metabolites into mucosal tissue compartments, subsequently

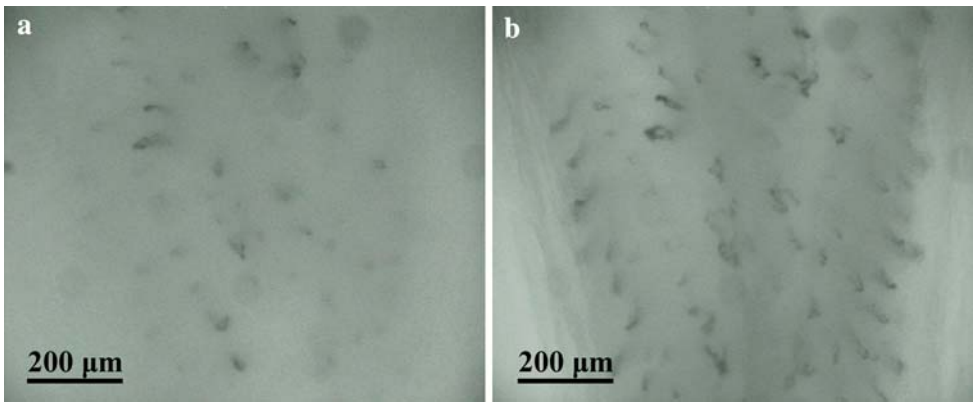

Fig. 2 Sidestream dark-field imaging of rabbit anterior maxillary gingiva before (**a**) and 30 min after chemotherapy intervention (**b**) in the allometric dose group (AD: CTX 34.3 mg/kg, MTX 2.3 mg/kg, 5-FU 34.3 mg/kg)

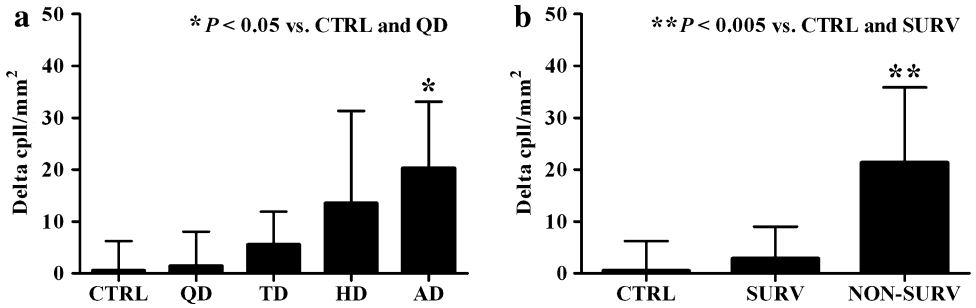

Fig. 3 Changes (delta) in gingival capillary density in each intervention group (**a**). Measurements were performed before and 30 min after chemotherapy or saline interventions. Changes (delta) in capillary density in control, survivor, and non-survivor animals (**b**). *CTRL* control, *QD* quarter allometric dose, *TD* third allometric dose, *HD* half allometric dose, *AD* allometric dose, cpll/mm^2: units for capillary density

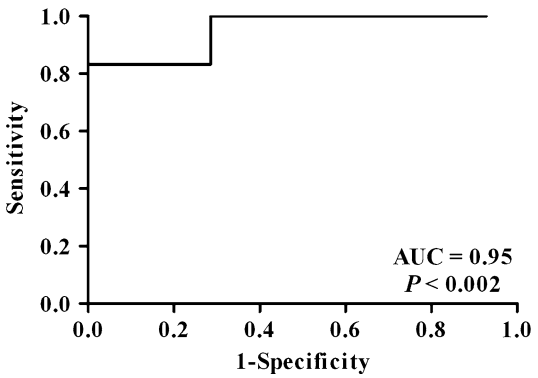

Fig. 4 Receiver operating characteristic (ROC) curve for predicting the outcome of acute changes (delta) in gingival capillary density with survival after 30 min of chemotherapy intervention. *AUC* area under the curve

triggering a cascade of cellular and molecular events responsible for oral mucosal barrier disturbances in oral complications.

In conclusion, this is the first study to describe the acute effects of CT on gingival microcirculation using SDF imaging. A simple, noninvasive and reproducible model to evaluate the applicability of SDF imaging for measuring changes in oral mucosal microcirculation following CT intervention, made it possible to demonstrate changes in gingival tissue perfusion in vivo. SDF imaging may be a useful tool for investigating the dose-dependent effects of cytostatic agents in oral microcirculation and may provide valuable information on the role of microvascular networks in CT-related oral complications and the treatment of oral tumors.

Acknowledgments We thankfully acknowledge professor Dr. M. A. Pokras from Tufts University for reviewing our drug scaling calculations. We are grateful to Dr. H. A. Griffioen and Dr. W. J. Florijn for their valuable advice on anesthesia in our animals and Mr. K. W. Meyer for biotechnical support. This project was funded by Novartis Pharmaceuticals Inc., Basel, Switzerland.

References

1. Bottini A, Berruti A, Bersiga A, Brizzi MP, Allevi G, Bolsi G, Aguggini S, Brunelli A, Betri E, Generali D, Scaratti L, Bertoli G, Alquati P, Dogliotti L (2002) Changes in microvessel density as assessed by CD34 antibodies after primary chemotherapy in human breast cancer. Clin Cancer Res 8:1816–1821
2. Capello V (2006) The dental suite: equipment needed for handling small exotic mammals. J Exot Pet Med 15:106–115
3. Dubin A, Pozo MO, Ferrara G, Murias G, Martins E, Canullan C, Canales HS, Kanoore EV, Estenssoro E, Ince C (2009) Systemic

and microcirculatory responses to progressive hemorrhage. Intensive Care Med 35:556–564
4. Elbers PW, Ozdemir A, van IM, van Dongen EP, and Ince C (2009) Microcirculatory imaging in cardiac anesthesia: ketanserin reduces blood pressure but not perfused capillary density. *J.Cardiothorac.Vasc.Anesth.*, 23, 95–101
5. Genot-Klastersky MT, Klastersky J, Awada F, Awada A, Crombez P, Martinez MD, Jaivenois MF, Delmelle M, Vogt G, Meuleman N, Paesmans M (2008) The use of low-energy laser (LEL) for the prevention of chemotherapy- and/or radiotherapy-induced oral mucositis in cancer patients: results from two prospective studies. Support Care Cancer 16:1381–1387
6. Gianni L, Baselga J, Eiermann W, Porta VG, Semiglazov V, Lluch A, Zambetti M, Sabadell D, Raab G, Cussac AL, Bozhok A, Martinez-Agullo A, Greco M, Byakhov M, Lopez JJ, Mansutti M, Valagussa P, Bonadonna G (2009) Phase III trial evaluating the addition of paclitaxel to doxorubicin followed by cyclophosphamide, methotrexate, and fluorouracil, as adjuvant or primary systemic therapy: European cooperative trial in operable breast cancer. J Clin Oncol 27(15):2474–2481
7. Gibbons G, Pokras M, Sedgwick C (1988) Allometric scaling in veterinary-medicine. Aust Vet Pract 18:160–164
8. Goedhart PT, Khalilzada M, Bezemer R, Merza J, Ince C (2007) Sidestream Dark Field (SDF) imaging: a novel stroboscopic LED ring-based imaging modality for clinical assessment of the microcirculation. Opt Express 15:15101–15114
9. Hahn KA (2005) Chemotherapy dose calculation and administration in exotic animal species. Semin Avian Exot Pet Med 14:193–198
10. Ince C (2005) The microcirculation is the motor of sepsis. Crit Care 9(Suppl 4):S13–S19
11. Isberg B, Paul C, Jonsson L, Svahn U (1991) Myocardial toxicity of high-dose cyclophosphamide in rabbits treated with daunorubicin. Cancer Chemother Pharmacol 28:171–180
12. Jensen SB, Mouridsen HT, Reibel J, Brunner N, Nauntofte B (2008) Adjuvant chemotherapy in breast cancer patients induces temporary salivary gland hypofunction. Oral Oncol 44:162–173
13. Lindeboom JA, Mathura KR, Harkisoen S, van den Akker HP, Ince C (2005) Effect of smoking on the gingival capillary density: assessment of gingival capillary density with orthogonal polarization spectral imaging. J Clin Periodontol 32:1208–1212
14. Lindeboom JA, Mathura KR, Ince C (2006) Orthogonal polarization spectral (OPS) imaging and topographical characteristics of oral squamous cell carcinoma. Oral Oncol 42:581–585
15. Lindeboom JA, Mathura KR, Ramsoekh D, Harkisoen S, Aartman IH, van den Akker HP, Ince C (2006) The assessment of the gingival capillary density with orthogonal spectral polarization (OPS) imaging. Arch Oral Biol 51:697–702
16. Meinders AJ, Elbers P (2009) Leukocytosis and sublingual microvascular blood flow. N Engl J Med 360:e9
17. Milstein DMJ, Lindeboom JAH, Ince C (2006) Sidestream dark-field imaging and image analysis of oral microcirculation under clinical conditions. In: Guilo A (ed) Anesthesia, Pain, Intensive Care and Emergency A.P.I.C.E. Springer-Verlag, Italy, pp 79–88
18. Sonis ST, Fey EG (2002) Oral complications of cancer therapy. Oncology (Williston Park) 16:680–686
19. Steeghs N, Gelderblom H, Roodt JO, Christensen O, Rajagopalan P, Hovens M, Putter H, Rabelink TJ, de Konning E (2008) Hypertension and rarefaction during treatment with telatinib, a small molecule angiogenesis inhibitor. Clin Cancer Res 14:3470–3476
20. Tsibiribi P, Bui-Xuan C, Bui-Xuan B, Lombard-Bohas C, Duperret S, Belkhiria M, Tabib A, Maujean G, Descotes J, Timour Q (2006) Cardiac lesions induced by 5-fluorouracil in the rabbit. Hum Exp Toxicol 25:305–309
21. Turek Z, Cerny V, Parizkova R (2008) Noninvasive in vivo assessment of the skeletal muscle and small intestine serous surface microcirculation in rat: sidestream dark-field (SDF) imaging. Physiol Res 57:365–371
22. Wauters J, Claus P, Brosens N, McLaughlin M, Malbrain M, Wilmer A (2009) Pathophysiology of renal hemodynamics and renal cortical microcirculation in a porcine model of elevated intra-abdominal pressure. J Trauma 66:713–719